

MS YA MIN (Orcid ID : 0000-0002-7526-4516)

PROF. HONGZHI KONG (Orcid ID : 0000-0002-0034-0510)

PROF. ELENA M. KRAMER (Orcid ID : 0000-0002-5757-1088)

Article type : MS - Regular Manuscript

Research article

A role for the Auxin Response Factors *ARF6* and *ARF8* homologs in petal spur elongation and nectary maturation in *Aquilegia*

Rui Zhang¹, Ya Min², Lynn D. Holappa², Cristina L Walcher-Chevillet^{2,3}, Xiaoshan Duan^{4,1}, Emily Donaldson², Hongzhi Kong¹, Elena M. Kramer^{2,*}

¹State Key Laboratory of Systematic and Evolutionary Botany, CAS Center for Excellence in Molecular Plant Sciences, Institute of Botany, Chinese Academy of Sciences, Beijing 100093, China

²Department of Organismic and Evolutionary Biology, Harvard University, 16 Divinity Ave., Cambridge, MA 02138, USA

³10x Genomics, 6230 Stoneridge Mall Road, Pleasanton, CA 94588-3260

⁴Harvard University Herbaria, Harvard University, 22 Divinity Ave., Cambridge, MA 02138, USA

*Author for correspondence: Elena M. Kramer; tel 1(617) 496-3460; fax 1(617) 496-5854; email ekramer@oeb.harvard.edu

This article has been accepted for publication and undergone full peer review but has not been through the copyediting, typesetting, pagination and proofreading process, which may lead to differences between this version and the [Version of Record](#). Please cite this article as [doi: 10.1111/NPH.16633](https://doi.org/10.1111/NPH.16633)

This article is protected by copyright. All rights reserved

Received: 22 January 2020

Accepted: 12 April 2020

Accession numbers: Aqcoe1G185500, Aqcoe3G431200, Aqcoe3G315800

Accepted Article

Summary

- The petal spur of the basal eudicot *Aquilegia* is a key innovation associated with the adaptive radiation of the genus. Previous studies have shown that diversification of *Aquilegia* spur length can be predominantly attributed to variation in cell elongation. However, the genetic pathways that control the development of petal spurs are still being investigated.
- Here, we focus on a pair of closely related homologs of the AUXIN RESPONSE FACTOR family, *AqARF6* and *AqARF8*, to explore their roles in *A. coerulea* petal spur development.
- Expression analyses of the two genes show that they are broadly expressed in vegetative and floral organs, but have relatively higher expression in petal spurs, particularly at later stages. Knockdown of the two *AqARF6* and *AqARF8* transcripts using virus-induced gene silencing (VIGS) resulted in largely petal-specific defects, including a significant reduction in spur length due to a decrease in cell elongation. These spurs also exhibited an absence of nectar production, which was correlated with down-regulation of *STYLISH* homologs that have previously been shown to control nectary development.
- This study provides the first evidence of *ARF6/8* homolog-mediated petal development outside the core eudicots. The genes appear to be specifically required for cell elongation and nectary maturation in the *Aquilegia* petal spur.

Key words: *Aquilegia*; Auxin Response Factor; cell elongation; nectary development; petal spur

Introduction

Spurs are tubular outgrowths of floral organs that typically contain nectaries and have evolved many times independently across the angiosperms to attract pollinators (Darwin, 1862; Hodges & Arnold, 1995; Moyroud & Glover, 2017). Nectar spurs show great variation in length, shape, orientation, and color, and have been regarded as key innovations that are highly associated with the increased species diversification in many lineages (Hodges *et al.*, 1995; Hodges, 1997a, b), although this association is not universal (Hodges *et al.*, 1995; Bastida *et al.*, 2010; Fernández-Mazuecos *et al.*, 2019). One particularly well understood case of spur evolution is found in the basal eudicot *Aquilegia* (columbine) of the buttercup family Ranunculaceae, one of two instances of spur evolution in the family. *Aquilegia* has nectar spurs on all five petals that vary dramatically in length across species, ranging from 1 to 15 cm (Munz, 1946). Previous studies have found that pollinator shifts from bees to hummingbirds, and hummingbirds to hawkmoths are the main driving force for the evolution of increased petal spur lengths among North American species (Whittall & Hodges, 2007). This particular evolutionary pattern, in conjunction with other floral morphological characters such as color, has promoted widespread distribution and rapid radiation of the genus over relatively short time scales, ~6 mya (Hodges & Arnold, 1994; Hodges *et al.*, 1995; Hodges, 1997a, b; Whittall *et al.*, 2007; Fior *et al.*, 2013). Therefore, understanding *Aquilegia* petal spur development and its underlying genetic controls will help us elucidate the mechanisms contributing to diversification of the genus.

Based on previous morphological studies, the development of the *Aquilegia* petal spur can be classified into two distinct phases. Beginning at stage 10 of floral development (floral meristem stages defined in Ballerini & Kramer, 2011; Min & Kramer, 2016), Phase I is characterized by localized cell divisions that promote the formation of an out-pocketing (i.e., the prepatterned spur cup) close to the base of the concave petal (Tucker & Hodges, 2005; Puzey *et al.*, 2011; Yant *et al.*, 2015; Min *et al.*, 2016). Phase II begins when the spur reaches 5–9 mm and is marked by a cessation of cell division and the initiation of anisotropic cell elongation, which then generates most of the final length of the organ (Puzey *et al.*, 2011). Comparisons among several species with

a wide range of spur lengths suggest that it is this second phase of cell elongation, especially the duration of the cell elongation period, that accounts for the majority of interspecific variation in spur-length (Puzey *et al.*, 2011). During the last stages of spur maturation, nectar is released from the nectary tissue through rupture of epidermal cell walls, and accumulates in petal spur tip (Anton & Kamińska, 2015; Min *et al.*, 2016).

Some progress has been made to understand the genetic control of *Aquilegia* spur development. The identity of the petal itself is specifically controlled by a subfunctionalized copy of *APETALA3* (*AP3*) termed *AqAP3-3*, whose protein product works together with the homologous *PISTILLATA* (*PI*) protein, *AqPI* (Kramer *et al.*, 2007; Sharma *et al.*, 2011). Transcriptome sequencing of dissected spur cups and petal blades found no evidence of expression of the *KNOTTED1-LIKE HOMEODOMAIN* (*KNOX*) family genes (Yant *et al.*, 2015), unlike what has been observed in the independently derived spurs of the core eudicot species *Linaria vulgaris* and monocot species *Dactylorhiza fuchsia* (Golz *et al.*, 2002; Box *et al.*, 2011, 2012). Instead, the Yant *et al.* (2015) study highlighted a potential role for later stage sculpting of localized cell divisions via pathways involving cell division inhibition factors such as *TEOSINTE* *BRANCHED1/CYCLOIDEA/PCF 4* (*TCP4*), and cell division promoters such as *ANGUSTIFOLIA* (*AN3*) and *JAGGED* (*JAG*) (Yant *et al.*, 2015; Min *et al.*, 2016). Also implicated were auxin signaling pathway genes (Yant *et al.*, 2015), such as members of the *STYLISH* (*STY*), *AUXIN RESPONSE FACTOR* (*ARF*), and *Aux/IAA* families, which are known to play pleiotropic roles in plant lateral organ development (Galun, 2010). Surprisingly, however, the first auxin-related candidate genes to be investigated, *AqSTY1*, *AqSTY2* and *AqLATERAL ROOT PROMORDIUM* (*AqLRP*), do not control overall spur development but rather promote nectary formation (Min *et al.*, 2018). Further, although *Arabidopsis* *STY1* largely acts through genes involved in auxin synthesis, such as members of the *YUCCA* family (Kuusk *et al.*, 2006), *YUCCA* homologs show no enrichment in *Aquilegia* spurs (Yant *et al.*, 2015). These findings suggest that, unlike the independently derived nectaries in the core eudicots that are controlled by homologs of the *YABBY* family gene *CRABS CLAW* (*CRC*) (Brown, 1938; Lee *et al.*, 2005), *Aquilegia* uses a completely separate genetic mechanism (*STY* family members) to control nectary specification (Min *et al.*,

2018). This is underscored by the fact that *AqCRC* is not expressed in *Aquilegia* nectaries (Lee *et al.*, 2005), while the *STY* genes are not expressed in *Arabidopsis* nectaries (Kuusk *et al.*, 2006).

In the current study, we have focused on another set of auxin-related candidate genes, the *Aquilegia ARF* homologs *AqARF6* and *AqARF8*, because they show significantly higher expression levels, as defined by the fragment per kilobase per million mapped fragments (FPKM), in the transcriptome of petal spur cups relative to that of petal blades (Yant *et al.*, 2015). Both of them encode members of the ARF family of transcription factors, which are core effectors in the auxin signaling pathway (Chapman & Estelle, 2009). In *Arabidopsis*, *ARF6* and *ARF8* redundantly mediate auxin-induced gene activation and promote jasmonic acid (JA) production (Ulmasov *et al.*, 1999a; Nagpal *et al.*, 2005). In particular, *arf6 arf8* double mutants, or plants over-expressing their negative regulator *MIR167*, exhibit stunted flowers with obviously shorter petals, stamen filaments, and smaller nectaries, which can be attributed to the decreased JA levels and ectopic expression of *KNOX* genes (Nagpal *et al.*, 2005; Wu *et al.*, 2006; Tabata *et al.*, 2010; Reeves *et al.*, 2012). In *Solanum pimpinellifolium*, ectopic expression of the *Arabidopsis* miR167a resulted in the similar phenotypes as those of the *Arabidopsis arf6 arf8* double mutants (Liu *et al.*, 2014), suggesting that the *ARF6/8*-like genes may have broadly conserved and redundant functions in promoting the growth of floral organs. These findings, together with the fact that potential protein interaction partners of *AqARF8*, the homologs of *SHORT HYPOCOTYL 2 (SHY2)* and *BIGPETAL (BPE)* (Szécsi *et al.*, 2006; Varaud *et al.*, 2011; Vernoux *et al.*, 2011), all show enriched expression in petal spur cups (Yant *et al.*, 2015), imply that *AqARF6* and *AqARF8* could have essential roles in the development of petal spurs.

To test this hypothesis, we studied their expression patterns and functional properties in the evo-devo model species *A. coerulea*. We found that although the two genes are broadly expressed, they do exhibit a degree of enriched expression in the developing petal spur. Consistent with this, double knockdown of the transcripts resulted primarily in petal defects, with the strong phenotypes showing a significant reduction in spur length due to a decrease in cell elongation rather than cell division, and the absence of nectar in the spur. In this system, the failure of nectary maturation is

correlated with down-regulation of the nectary identity paralogs *AqSTY1* and *AqSTY2* (collectively referred to as *AqSTY1/2*) (Min *et al.*, 2018), suggesting that *AqARF6/8* function to maintain their expression, possibly via a conserved role for jasmonate in nectary function.

Materials and Methods

Plant materials and growth conditions

Seeds of *Aquilegia coerulea* E. James ‘Origami Red & White’ were sown in nutrient soil and grown in the growth chamber under conditions of 14 h-day/10 h-night at 18/13°C and 40% relative humidity. After two months, plants with four to six true leaves were vernalized at 4 °C for 4 weeks. One day after the plants had been removed from vernalization, they were subjected to virus induced gene silencing (VIGS) treatment as described in (Sharma & Kramer, 2013).

Identification and isolation of candidate genes

Total RNA was extracted from inflorescences by using PureLink Plant RNA Reagent (Life Technologies) and treated with Turbo DNase (Ambion). cDNA was then reverse-transcribed from 1µg of total RNA using SuperScript II First-Strand Synthesis System (Life Technologies), which was then used as the template to amplify the cDNA sequences of *AqARF6* (Aqcoe1G185500) and *AqARF8* (Aqcoe3G431200). Amplified fragments were purified and cloned into TOPO-TA cloning[®] vector (Life Technologies) for sequencing. Gene-specific primers used for genes isolation are listed in Table S1.

Phylogenetic analysis

To confirm the orthology of *AqARF6*, *AqARF8*, and *AqBPE* (Aqcoe3G315800), coding sequences of the genes from representative species were retrieved through BLAST searches against the available databases (Table S2, Table S3). Phylogenetic analysis was performed for the alignable DNA sequences in PhyML3.0 using the maximum-likelihood method (Guindon *et al.*, 2010). The general time reversible (GTR) + I + Γ model was applied and 1,000 bootstrap

replicates were performed. The final resultant tree was displayed by MEGA7.0 (Kumar *et al.*, 2016).

Real-time quantitative polymerase chain reaction (RT-qPCR)

RT-qPCR experiments were conducted for investigation of the expression patterns of *AqARF6* and *AqARF8* in *A. coerulea*, as well as the silencing efficiency of the VIGS experiments. Total RNAs were isolated from inflorescences and dissected floral organs from F1 to F4 for expression profile analyses, as well as from mature sepals and petals for silencing efficiency analyses. RNAs were DNase treated and reverse-transcribed as described in (Min *et al.*, 2016; Min *et al.*, 2018). The resulting cDNAs were diluted 1:20 as templates. RT-qPCR was conducted using the PerfectCTa SYBR Green FastMix, Low ROX (Quanta Biosciences) in the Stratagene MX3005P Real-Time PCR System. At least four biological replicates per sample, each with three technical replicates, were assayed. Relative gene expression values were calculated using the comparative CT ($2^{-\Delta\Delta CT}$) method (Livak & Schmittgen, 2001), with the *AqIPP2* (*ISOPENTYL PYROPHOSPHATE: DIMETHYLALLYL PYROPHOSPHATE ISOMERASE2*) gene being used as an internal control (Sharma *et al.*, 2011). Primers used in this study were provided in Table S1.

Locked nucleoid acid *in situ* hybridization (LNA-ISH)

LNA-ISH was utilized to visualize the expression patterns of *AqARF6* and *AqARF8* because conventional RNA *in situ* hybridization had failed. LNA probes were chosen because they have been demonstrated to bind to RNA with unprecedented affinity and specificity (Petersen & Wengel, 2003). For this reason, two double Digoxigenin labeled LNA probes (labeled at the 5' and 3' end) specific to *AqARF6* and *AqARF8* were designed using the platform <https://www.exiqon.com/oligo-tools> (Exiqon). Fixation and embedding of the inflorescences and floral buds followed the procedures as described in (Kramer, 2005).

LNA-ISH was conducted with a modified protocol from (Kramer, 2005) and (Javelle & Timmermans, 2012). *In situ* slides were cleared with Citrisolv (Fisherbrand) twice for 10 min, and then rehydrated in an ethanol series. After a wash in 1× phosphate buffer saline (PBS) solution,

the slides were digested with Pronase at 37°C for 20 min. The slides were washed twice with 1× PBS, dehydrated in an ethanol series, and allowed to air dry for 10 min. LNA probes were applied onto the slides by mixing 5 µL of 100 µM stock probe into 200 µL of hybridization solution. The hybridization solution-probe mix was incubated at 80°C water bath for 2 min and then was applied onto a slide sandwich, which were thereafter incubated overnight in a humid chamber (54°C). The hybridized slides were separated and washed in decreasing concentrations of saline-sodium citrate (SSC) buffer (5×, 1×, 1×, 0.2×, 0.2×) at 55°C water bath for 30 min per step. The remaining treatment of the slides just followed the procedures as described before (Kramer, 2005). Sections were then counterstained with calcofluor and imaged using a combination of white and fluorescent light by the Zeiss AxioImager microscope.

Virus-induced gene silencing (VIGS)

The VIGS experiment was performed according to protocols described in Gould & Kramer (2007). Fragments of *AqARF6* (299 bp), *AqARF8* (298 bp) and *AqANTHOCYANIDIN SYNTHASE* (*AqANS*) (414 bp) were introduced into the tobacco rattle virus 2 (TRV2) vector to generate the TRV2-*AqARF8-AqARF6-AqANS* construct, in which the *AqANS* fragment was used as the marker of gene silencing. These constructs were transformed into GV3101 electrocompetent *Agrobacterium* cells. 482 vernalized plants from 4 batches and 175 vernalized plants from 2 batches were treated with TRV2-*AqARF8-AqARF6-AqANS* and TRV2-*AqANS* constructs, respectively. Flowers showing silencing phenotypes were photographed using a Canon X type digital SLR camera (Canon, Melville, NY, USA), and the length and width of silenced floral organs were measured.

Cell counts and measurements

WT and strong silenced mature petals were fixed in FAA, and then transferred to 50% ethanol. Petals were cut longitudinally through the attachment point and spur tip, mounted on a glass slide with water and imaged as quickly as possible. Overlapping images were taken at the 20× magnification along the entire length of the petal by using the Zeiss AxioImager microscope. A composite image was created by stitching individual images together by using Adobe

Photoshop CS3. The cell number was counted along the axis from the tip of petal blade to that of petal spur. Meanwhile, the length $l(s)$ and width $w(s)$ of each counted cell were also measured by using ImageJ. The cell size was characterized by cell area $A(s) = lw$, while cell shape was characterized by cell anisotropy $E(s) = l(s)/w(s)$ (Puzey *et al.*, 2011).

Scanning electron microscopy (SEM) and histology

WT and strongly silenced mature petals were fixed in FAA, dehydrated in an ethanol series. For SEM, samples were dried with a CO₂ critical-point dryer. Dried, uncoated petals were mounted and imaged with a JEOL JSM-6010 LC Scanning Electron Microscope S-4800 scanning electron microscope. For histology, samples were dehydrated in an ethanol series and then embedded in Paraplast Plus (Oxford Labware, St Louis, MO, USA). Tissues were sectioned to 8 μm and stained with 0.5% toluidine blue, and then imaged the pictures by using the Zeiss AxioImager microscope.

Yeast two-hybrid analyses

The GAL4-based MATCHMAKER Two-Hybrid System (Clontech, Palo Alto, CA, USA) was used to determine the protein-protein-interactions (PPIs). For the four loci, *AqARF6*, *AqARF8*, *AqSHY2*, and *AqBPE*, full-length open reading frames (ORFs) were used for constructing the pGADT7 vector, while for constructing the pGBKT7 vector, full length ORFs were used for *AqSHY2* and *AqBPE* but partial ORFs encoding only the protein interactions domains III and IV were used for *AqARF6* and *AqARF8*. This was necessary due to the fact that ARF6 and ARF8 contain transcriptional activation domains in their N-termini (Ulmasov *et al.*, 1999a) All constructs were transformed into yeast (*Saccharomyces cerevisiae* strain AH109) competent cells using the LiAc Yeast transformation procedure following the manufacturer's instructions (Sigma Aldrich, St. Louis, MO). To check for auto-activation, yeast transformant for each construct was tested for growth on the selective synthetic dropout (SD) media lacked either His, Leu, Trp (-HLT) or Ade, His, Leu, Trp (-AHLT) supplemented with 0, 10, 20, and 30 mM 3-amino-1,2,4-aminotriazole (3-AT, Sigma Aldrich, St. Louis, MO). We found that auto-activation was eliminated on the -AHLT SD media supplemented with 10 mM 3-AT. For the

test of PPIs, transformants carrying both AD and BD constructs were tested for growth on the – HLT or –AHLT SD media supplemented with 0, 10, 20, and 30 mM 3-AT at 28 °C for 4 days. Experiments were repeated two times, with the empty-vector transformants being used as negative controls and the *A. thaliana* AP3 and PI used as positive controls.

Application of Auxin

Indole-3-acetic acid (IAA; Alfa Aesar, Tewksbury, MA) was dissolved in liquid lanolin (40°C) to reach a final concentration of 10 mM, allowed to cool to room temperature, and the paste was applied to surface of organs using a surgical needle. A total of 75 flowers from 23 individual plants were treated. For each treatment, flowers were subdivided into two groups evenly, and the paste was applied to: 1) the outer surface of petal spurs, and 2) the inner surface of petal spurs. For flowers received petal treatments, two to three sepals were removed for the convenience of application. All flowers were treated at approximately the same size and developmental stage, of which the petals were about 0.3-0.5 cm in length.

Application of JA and JA inhibitor

(±)-Jasmonic Acid (JA; Cayman Chemical, MI) and JA inhibitor 1-phenyl-3-pyrazolidinone (Phenidone; Sigma-Aldrich, MO) were dissolved in ethanol and diluted to desired concentrations with distilled water. Prior to application, nectar volumes of three petals of a blooming flower were measured, then nectar were emptied by using a thin strip made from kimwipe. Subsequently, petal spurs were immersed in 1) distilled water as control, 2) 1 mM JA, 3) 5 mM JA, or 4) 2 mM JA inhibitor solutions for 30 seconds. The nectar volumes of these emptied petal spurs were measured every eight hours. Flowers were treated at the approximately the same developmental stage, when the anthers of the inner most whorl of stamens were just starting to dehisce.

Results

Identification of *AqARF6* and *AqARF8*

The putative *ARF6* and *ARF8* homologs were identified from the *A. coerulea* genome, with

each represented by a single copy and referred to as *AqARF6* and *AqARF8*, respectively (Fig. S1). The *AqARF6* gene has 14 exons with 2,508 base pairs encoding 836 amino acid residues, while *AqARF8* has 15 exons with 2,538 base pairs encoding 846 residues (Fig. S1). Consistent with the structure of ARF6- and ARF8-like proteins from representative species of seed plants, both *AqARF6* and *AqARF8* contain four well-conserved domains that characterize the ARF family (Fig. S1, S2). Specifically, the N-terminal region includes a B3 domain and an ARF domain involved in DNA-binding, and the C-terminal region includes the so-called III and IV domains that are involved in dimerization (Finet *et al.*, 2012; Mutte *et al.*, 2018).

To further confirm the orthology of the two genes, a maximum-likelihood phylogenetic tree was constructed for 22 *ARF6/8*-like genes from eight representative species of seed plants, using 12 homologs of *ARF5/7*-like genes as outgroup (Fig. S3). In line with previous studies (Remington *et al.*, 2004; Finet *et al.*, 2012; Mutte *et al.*, 2018), the gymnosperm *Ginkgo biloba* possesses only one *ARF6/8*-like homolog, which was resolved as sister to the remaining 21 angiosperm genes. These sequences fall into two strongly supported clades corresponding to *ARF6*- and *ARF8*-like genes, each containing homologs from *Amborella* as well as monocots and eudicots. This indicates that the duplication that produced the paralogous *ARF6*- and *ARF8*-like lineages likely occurred after the divergence of the gymnosperms but before the diversification of the angiosperms. As expected, *AqARF6* and *AqARF8* fall into the *ARF6* and *ARF8* clades, respectively, confirming their orthology.

***AqARF6* and *AqARF8* are broadly expressed during vegetative and reproductive growth**

To understand the expression patterns of *AqARF6* and *AqARF8* in *A. coerulea*, we first performed real-time quantitative polymerase chain reaction (RT-qPCR). We prepared RNA samples from seedlings, leaves, inflorescences, as well as dissected floral organs grouped into pools termed F1 to F4 (Fig. 1a-e). F1 flowers had spurs of 0.2 – 0.4 cm, consistent with Phase I of spur development (Fig. 1B); F2 flowers had spurs of 0.5 – 0.9 cm, consistent with the transition from Phase I to Phase II (Fig. 1C); F3 flowers had spurs of 1.5 – 2.0 cm, consistent with Phase II of spur development (Fig. 1D); and F4 flowers corresponded to the mature anthesis stage (Puzey

et al., 2011). The petals were further dissected into petal blades and petal spurs, which correspond, respectively, to the parts above and below the attachment point of the petal. We found that both genes are expressed in all of the investigated tissues (Fig. 1f-g), suggestive of broad expression during vegetative and reproductive growth. We also found that *AqARF8* has generally higher expression levels than *AqARF6* in all of the samples (Fig. 1f-g). Notably, both *AqARF6* and *AqARF8* show increased expression in F4 sepals relative to earlier stages (Fig. 1f-g), and *AqARF8* shows higher expression levels in the petal spurs relative to the blades at later stages (Fig. 1g).

To further obtain detailed spatiotemporal expression patterns of *AqARF6* and *AqARF8* in early stages of flower development, we conducted Locked Nucleic Acid *in situ* hybridization (LNA-ISH) experiment, as the conventional *in situ* hybridization technique could not detect clear expression signals for the two transcripts. Our results show that the expression patterns of these genes are largely overlapping. At floral meristem stage 3 when the sepal primordia initiate (Min *et al.*, 2016), their expression signals are diffuse in the floral meristem (Fig. 2a,e). At stage 6, the genes remain strongly expressed in all floral primordia (Fig. 2b,f), but by stage 9, expression has declined in the staminodes while it remains strong in the petals, stamens and carpels (Fig. 2c,g). By stage 10, when the petal spur cups are forming, the expression of these transcripts can still be detected in the whole petals, especially the spur cup (Fig. 2d,h).

Silencing of *AqARF6* and *AqARF8* predominately results in shortened petals with a decrease in cell length

To investigate the functions of *AqARF6* and *AqARF8* in *A. coerulea*, we performed TRV-based VIGS experiments. We amplified ~300 bp fragments of the two loci and introduced them into a TRV2 vector that already contained a fragment of *Aquilegia AqANS* (TRV2-*AqANS*) to generate the TRV2-*AqARF8-AqARF6-AqANS* construct. This construct was used to simultaneously silence the three genes, with the *AqANS* as the marker of gene silencing. Dual silencing of *AqARF6* and *AqARF8* was immediately pursued because single copy mutants in *Arabidopsis* have no loss-of-function phenotypes (Ulmasov *et al.*, 1999a; Nagpal *et al.*, 2005). In addition, separate experiments were performed using TRV2-*AqANS* as a positive control. We

found that the TRV2-*AqANS* silenced plants displayed no visible morphological change except for loss of anthocyanin. However, across four batches of TRV2-*AqARF8-AqARF6-AqANS* treatments (almost 500 plants), we obtained 36 flowers from 23 plants that showed *AqANS* silencing as well as petal-specific morphological phenotypes (Fig. 3). RT-qPCR was used to assess the degrees of target gene silencing (Fig. S4). Mature sepals and petals showing what we termed moderate (*arf_m*) and strong (*arf_s*) phenotypes were collected, and compared to TRV2-*AqANS* strongly silenced (*ans_s*) sepals and petals. The results show that the expression levels of *AqARF6* and *AqARF8* were reduced by approximately 80% in both sepals and petals relative to controls, indicating that the silenced phenotypes were indeed the result of down-regulation the two transcripts.

Of the TRV2-*AqARF8-AqARF6-AqANS* silenced plants with *arf_s* and *arf_m* phenotypes, the most conspicuous change was the smaller size of petals (Fig. 3a-h). To better understand the nature of this reduced size, we compared the length and width of petals between *AqARF6/8*-silenced petals and controls. We found that the *arf_s* petals show no significant decrease in width (Fig. 3i). However, the *AqARF6/8*-silenced petals were significantly shorter than that of controls, with their lengths averaging 3.48 cm in *arf_s* petals and 4.88 cm in *ans_s* petals, respectively (Fig. 3j, $P = 3.73 \cdot 10^{-17}$). This reduced petal length was not due to the blade length variation (1.25 cm in *arf_s* petals compared with 1.21 cm in *ans_s* petals, $P = 0.47$) but, rather, differences in spur length (2.23 cm in *arf_s* petals compared with 3.67 cm in *ans_s* petals, $P = 1.36 \cdot 10^{-25}$), amounting to a 39% reduction (Fig. 3k-l). In addition, to determine whether the sizes of the other floral organs were affected, we also measured the width and length of sepals, as well as the length of stamens, staminodes, and carpels between *AqARF6/8*-silenced flowers and controls. We found no significant differences between the silenced and control organs for sepal width and length or carpel length (Fig. S5a-c,f). The lengths of the stamens and staminodes in *arf_s* flowers are indeed significantly reduced ($P = 0.001$), but the degree of reduction is smaller, less than 20% (Fig. S5d-e). These results suggest that silencing of *AqARF6* and *AqARF8* led to shorter floral organs, with the strongest effect being in the petal spurs.

We next sought to determine whether the reduction in *arf_s* spur length was due to the variation in cell number, cell size, cell shape, or some combinations of these factors. To answer this question, we measured longitudinal cell counts, individual cell width (*w*) and length (*l*), cell area, and cell anisotropy (*l/w*) for six wild type (WT) and six *arf_s* petals (Fig. 4). We found that the average cell number did not significantly differ between WT and *arf_s* petals (Fig. 4c), whereas the accumulative and average cell length (Fig. 4d-e, $P = 1.32 \cdot 10^{-4}$ and $P = 1.34 \cdot 10^{-5}$, respectively), as well as cell anisotropy (Fig. 4f, $P = 6.47 \cdot 10^{-4}$) were significantly decreased in *arf_s* petals relative to WT. We also found a reduction in petal cell width (Fig. S6a, $P = 0.004$) and, consistent with these findings, a coordinate reduction in cell area in *arf_s* petals (Fig. S6c, $P = 1.85 \cdot 10^{-5}$). More importantly, we also observed a clear pattern that the differences in cell length and anisotropy between WT and *arf_s* petals were most pronounced closer to the nectary (Figs 4g-h; S6b,d). Taken together, these results provide strong evidence that the *AqARF6/8* contribute the petal spur growth by promoting cell expansion rather than cell division.

Silencing of *AqARF6* and *AqARF8* impacts nectary maturation

Another interesting observation is that all of the *arf_s* petal spurs and most of those from *arf_m* flowers appeared to lack nectar compared to the controls (Fig. 5a-f). We observed a total loss of nectar production in *arf_s* petals, as measured as a percentage of spur volume occupied (Fig. 5g), suggestive of defects in nectary maturation. Further inspection of the macro- and micro-structures of the spur tips revealed some morphological and anatomical defects in the *arf_s* petals. First, under the scanning electron microscopy (SEM), WT spurs terminate in a bulbous nectary that actively secretes nectar starting at stage 12, when all the floral organs reach their final lengths (Ballerini & Kramer 2011; Min *et al.*, 2016), and the inner surface contains secretory residues (Fig. 5h-j; Min *et al.*, 2018). The presumptive nectary region of *arf_s* spur tips, however, did not become inflated and the inner surface revealed a complete lack of the telltale signs of nectar secretion (Fig. 5l-n). Second, histological sectioning revealed that, compared to WT nectaries, *arf_s* spur tips showed some differentiation of the inner/adaxial epidermis lining the nectary, consistent with that observed in WT spur tips. However, the underlying parenchyma cells

of the *arf_s* spur tips were qualitatively more disorganized, with more highly expanded and distorted shapes as compared with WT (Fig. 5k,o).

The loss of nectar production observed in *AqARF6/8*-silenced petals is similar to what has been found in *A. coerulea* petals simultaneously silenced for the three STY family genes, *AqSTY1*, *AqSTY2* and *AqLRP* (Min *et al.*, 2018). To understand the regulatory relationships between the *AqARF6/8* and the *STY* loci, we assessed the expression of the three *AqSTY*-like genes in *AqARF6/8*-silenced petals. *AqSTY1* and *AqSTY2* were indeed down-regulated, with the degree of *AqSTY2* silencing being more evident (Fig. 5p-q).

AqARF6 and AqARF8 interact with AqSHY2 but not with AqBPE in yeast

When auxin is absent, the Arabidopsis ARF proteins form heterodimers with members of the Aux/IAA family of negative regulatory co-factors (Guilfoyle & Hagen, 2007; Vernoux *et al.*, 2011). In addition, it has been reported that the Arabidopsis ARF8 protein represses petal growth by interacting with a bHLH family transcription factor BPEp, which is the product of a petal-specific transcript of the *BPE* locus (Varaud *et al.*, 2011). The main, or “ubiquitous”, transcript of *BPE* is termed *BPEub* and the capacity of BPEub to interact with ARF8 has not been reported. Interestingly, it has been found that the putative *SHY2* and *BPE* homologs in *Aquilegia*, named *AqSHY2* and *AqBPE*, respectively, exhibit significantly enriched expression in petal spurs relative to petal blades, coincident with the differential expression of *AqARF6* and *AqARF8* in these tissues (Yant *et al.*, 2015). However, it is important to note that the *AqBPE* transcript corresponds to Arabidopsis *BPEub* and a *BPEp* transcript variant has not been detected in the *Aquilegia* transcriptome (Fig. S7). Furthermore, in the context of our phylogenetic analysis confirming the orthology of *AqBPE*, we discovered that there do not appear to be any *BPEp* transcripts annotated for any homolog outside the Brassicaceae (Fig. S7). Given that the interaction of BPEub and ARF8 has not been previously reported, we tested two-way interactions among AqARF6, AqARF8, AqSHY2, and AqBPE by using yeast two-hybrid (Y2H) assays. Our results show that both AqARF6 and AqARF8 can interact with AqSHY2 (Table 1; Fig. S8), consistent with an evolutionary conservation of these interactions. No interaction was observed

between AqARF8 and AqBPE (or between AqARF6 and AqBPE; Table 1; Fig. S8).

Hormonal effects on spur and nectary development

In order to further explore the roles of auxin in petal spur development, we performed exogenous application of indole-3-acetic acid (IAA) to wildtype petals at stage 11B of floral development, which is when petal spurs first become visible between the sepals and the earliest possible treatment stage (Fig. S9) (Min *et al.*, 2016). Lanolin applied to petals as controls did not reveal any prominent morphological change in the petals (Fig. S9c-d), which exhibited smooth outer epidermal cells and well-organized inner mesophyll cells (Fig. S9e-f). However, application of 10 mM IAA either inside or outside of petal spurs resulted in twisted laminae (Fig. S9g-h,l-m). SEM and histological analyses showed that the dramatic distortions were the result of over- and/or uncoordinated proliferation of lamina tissue (Fig. S9i-k,n-o). Moreover, no nectariferous tissue was observed in the distorted region of the IAA treated petal spurs (Fig. S9o). These findings are in line with the observations that overall increase in free auxin in *Aquilegia* and Arabidopsis flowers did not produce longer floral organs and nectaries (Nagpal *et al.*, 2005; Min *et al.*, 2018), suggesting that the much more limited phenotype observed in *arf_s* petals reflects only a facet of auxin-responsive phenotypes in *Aquilegia* petals.

It has been shown that JA production in flowers of the Brassicaceae requires the expression of *ARF6* and *ARF8*, which can promote petal growth and nectar secretion (Ulmasov *et al.*, 1999a; Nagpal *et al.*, 2005; Radhika *et al.*, 2010). We, therefore, investigated the effect of exogenous jasmonic acid (JA) and its inhibitor phenidone on nectar secretion in emptied petal spurs of *A. coerulea*. We found that treatment with JA, phenidone, and control showed no obvious difference in nectar refilling rate or final nectar volume (Fig. S10a-b). We further examined the expression of the genes homologous to the Arabidopsis *ALLENE OXIDE SYNTHASE (AOS)*, *DEFECTIVE IN ANther DEHISCENCE1 (DADI)*, and *ALLENE OXIDE CYCLASE4 (AOC4)*, which are all involved in JA biosynthesis, in *arf_m* and *arf_s* tissues (Fig. S10c). These results were highly variable, with some silenced petals showing reduction while others are unchanged or even higher than the controls. Overall, a consistent difference in gene expression patterns was not detected, but

this may be due to the variable nature of VIGS.

Discussion

***AqARF6* and *AqARF8* are broadly expressed but primarily function in petal spur development**

In this study, we investigated the expression patterns and functions of *AqARF6* and *AqARF8* in *A. coerulea*. We found that the genes are broadly expressed throughout the plant, including seedlings, leaves, early floral meristems and all maturing floral organs (Figs. 1-2). These patterns are in line with those observed for their counterparts in *Arabidopsis* and tomato (Ulmasov *et al.*, 1999b; Nagpal *et al.*, 2005; Reeves *et al.*, 2012; Liu *et al.*, 2014), suggestive of conservation of *AqARF6*- and *AqARF8*-like gene expression across dicots. Mutation or knockdown of these genes in the same eudicot models generated shorter floral organs, particularly petals, stamens and carpels (Nagpal *et al.*, 2005; Reeves *et al.*, 2012; Liu *et al.*, 2014). Consistent with this, we observed that knockdown of *AqARF6* and *AqARF8* resulted in shortened petals, stamens and staminodes, although the greatest impact was on petal spur length. In addition, we recovered defects in nectary maturation that eliminated nectar secretion and reduced expression of the close paralogs *AqSTY1/2*.

Although these relatively narrow phenotypes may be surprising given the broad expression of *AqARF6* and *AqARF8*, there are several possible explanations. First and foremost, developing petal spurs may be more sensitive to the down-regulation of *AqARF6/8* than other floral organs (Fig. S4) because their spatio-temporal expression patterns are highly consistent with the development of petal spurs. At stage 10, for example, the two genes exhibit localized expression in the petal spur forming region (Fig. 2). After that, the transcripts, particularly that of *AqARF8*, maintain relatively higher expression levels in developing petal spurs than blades (Fig. 1), which is consistent with the fact that the petal spur maturation depends significantly on cell expansion (Puzey *et al.*, 2011). Second, functional redundancy among ARF family members has been broadly observed (Finet *et al.*, 2012). The *Aquilegia* genome does not contain homologs of *ARF7*

or *ARF19*, the next closest relatives of *ARF6/8* (Mutte *et al.*, 2018), but there is an *ARF5* homolog, which could potentially complement aspects of *AqARF6/8* function. Third, the *AqARF6/8* range of function could be narrowed by restricted expression of co-factors, including *AqSHY2*, which is also enriched in petal spurs (Yant *et al.*, 2015). Although we have ruled out conservation of the ARF8-BPEp interaction, several additional co-factors have been identified, including MYB77, which is yet to be investigated in *Aquilegia*. Last, but not least, *AqARF6* and *AqARF8* may be post-transcriptionally regulated by microRNAs, which can act to suppress either target RNA stability or translation. *ARF6* and *ARF8* homologs are targeted by miR167 across diverse plant species (Axtell & Bartel, 2005), and both an *AqMIR167* locus and its target sites in *AqARF6* and *AqARF8* have been identified in the *Aquilegia* genome (Fig. S1) (Puzey & Kramer, 2009). However, the expression and function of *AqMIR167* in regulating *AqARF6/8* is yet to be explored, including any possibility of post-translational regulation.

***AqARF6* and *AqARF8* promote petal spur elongation through anisotropic cell expansion**

Perhaps the most intriguing aspect of this study is that *AqARF6/8*-silenced plants showed obviously and significantly shorter petal spurs due to a decrease in cell elongation, especially in the region close to the nectary (Fig. 3). This result is consistent with the observations that simultaneous mutation or inactivation of the *ARF6/8*-like genes in *Arabidopsis* and tomato led to reduced inflorescence stem length and immature flowers with shorter petals, stamen filaments, and styles, whose cell lengths were similarly reduced relative to WT (Nagpal *et al.*, 2005; Liu *et al.*, 2014). Therefore, these results provide evidence that *ARF6/8*-like genes may have a conserved and redundant function in promoting cell expansion, which in turn, regulates the size of lateral organs. At the same time, our auxin application experiment suggests that petals have a much broader potential to respond to auxin than what is observed in *AqARF6/8*-silenced plants, reflecting that these loci only control a component of auxin response.

A previous study has found that *Aquilegia* spur elongation is predominantly driven by anisotropic cell expansion (Puzey *et al.*, 2011). Our results have demonstrated that *AqARF6/8*-silenced petals still show anisotropic cell expansion, but the degree of expansion is

reduced with a stronger effect on cell length than width. As noted above, it may be that the *arf_s* phenotype of spurs is so significant in petals because their development is much more dependent on cell elongation. At the same time, it seems likely that in addition to *AqARF6/8*, other genes contribute to petal spur elongation, which appears to be under polygenic control (Kramer & Hodges, 2010; Zhu *et al.*, 2014).

Moreover, it should be noted that in *Arabidopsis*, *ARF8* also has an opposing role in restricting cell expansion, as is seen in the larger petals observed in single *arf8* mutants, apparently due to its protein interaction with the BPEp protein (Varaud *et al.*, 2011). As discussed above, the *BPE* locus, a bHLH family member, has two alternatively spliced transcripts: the ubiquitously expressed *BPEub* and the petal-specific *BPEp*. Interestingly, it is the BPEp-specific C-terminal domain that confers the ability of BPEp to interact with ARF8, which in turn restricts the growth of petals (Varaud *et al.*, 2011). In *Aquilegia*, however, AqARF8 shows no such ability to interact with the AqBPE (Table 1; Fig. S8). Further inspection of the exon-intron structure reveals that all the transcripts of *AqBPE* are similar to that of *BPEub* rather than *BPEp*, meaning that they do not have the necessary C-terminal domain for ARF8 interaction (Fig. S7). More broadly, our finding that *BPEp*-like transcripts have not been detected outside the Brassicaceae highlights the need to study the function of the “ubiquitous” *BPEub* transcripts, both in *A. thaliana* and other model systems.

***AqARF6* and *AqARF8* control nectary maturation**

In this study, we also found that silencing of *AqARF6/8* led to immature nectaries that failed to secrete nectar (Fig. 5). These defects are correlated with a decrease in *AqSTY1/AqSTY2* expression, but the *arf_s* phenotypes are distinct from those observed in triple *AqSTY*-silenced flowers (Min *et al.*, 2018). In *AqSTY*-silenced petals, the spur tip was often highly misshapen with a complete failure to differentiate internal epidermal layers and a lack of the distinct color difference that is typically observed in WT spurs. In contrast, in the *arf_s* petals, the nectaries fail to properly expand but they are differentiated in color from the spur and have less severe disruption in cell differentiation (Fig. 5). These results suggest that *AqARF6/8*-silenced nectaries

initiate normally and may have early *AqSTY1/2* expression, but the nectaries do not become functional and *AqARF6/8* may be directly or indirectly required for the maintenance of *AqSTY1/2* expression. One potential candidate for this regulatory connection is the hormone jasmonate, which has been shown to regulate nectary maturation in other plant systems and to be under the control of *ARF6/8* function in *Arabidopsis* (Nagpal *et al.*, 2005; Radhika *et al.*, 2010; Reeves *et al.*, 2012). However, our investigation of jasmonate function in *Aquilegia* has been inconclusive. Application of the hormone and its inhibitor did not perturb secretion, although this negative result may be due to saturating endogenous production levels of the hormone. Likewise, we did not observe consistent down-regulation of jasmonate biosynthesis pathway loci, but this could be due to the variable nature of VIGS or a failure to consistently capture a key developmental stage.

It is fascinating to note that although nectaries have clearly evolved independently in the lineages leading to *Arabidopsis* and *Aquilegia* (Lin *et al.*, 2014) and their development is controlled by different master regulatory genes (*CRC* in *Arabidopsis* and *STY*-like genes in *Aquilegia*; Lee *et al.*, 2005; Min *et al.*, 2018), they share critical regulation by *ARF6/8* homologs. Further study is necessary to determine whether this may be due to conserved roles for *ARF6/8*, for instance in regulating jasmonate synthesis, which could function in a conserved fashion as a regulator of secretion, or possibly conserved roles in general floral maturation (Reeves *et al.*, 2012). Alternatively, the function of *ARF6/8* homologs in nectary development could be completely convergent in association with the independent evolution of these structures in the core and lower eudicots.

Acknowledgements

We thank Prof. Yi Ren at Shaanxi Normal University, Dr. Wengen Zhang at Jiangxi Agricultural University, the Kramer lab, and three anonymous reviewers for valuable comments. This work was supported by NSF award IOS-1456217 to E.K. and National Natural Science Foundation of China Grant 31930008 to H.K.

Author contributions

E.M.K., C.W-C., and R.Z. conceived the project. C.W-C. prepared the initial *in situ* and VIGS constructs. R.Z. carried out the sample collection, *in situ* hybridization experiment, and the RT-qPCR experiment. R.Z. and X.D. carried out the VIGS experiment. Y.M. performed the exogenous hormone applications and corresponding histology and SEM analyses. L.H. performed the protein-protein interaction experiments. E.D. performed initial phylogenetic and molecular analyses of *AqBPE*. R.Z., H.K. and E.M.K. contributed to the writing and revision of the manuscript.

ORCID

Rui Zhang: <https://orcid.org/0000-0002-2467-7222>

Xiaoshan Duan: <https://orcid.org/0000-0003-2462-8399>

Elena M. Kramer: <https://orcid.org/0000-0002-5757-1088>

Hongzhi Kong, <https://orcid.org/0000-0002-0034-0510>

References

Antoń S, Kamińska M. 2015. Comparative floral spur anatomy and nectar secretion in four representatives of Ranunculaceae. *Protoplasma*, **252**, 1587-1601.

Axtell MJ, Bartel DP. 2005. Antiquity of microRNAs and their targets in land plants. *The Plant Cell*, **17**, 1658-1673.

Ballerini E, Kramer EM. 2011. The control of flowering time in the lower eudicot model *Aquilegia*. *EvoDevo*, **2**:4.

Bastida JM, Alcántara JM, Rey PJ, Vargas P, Herrera CM. 2010. Extended phylogeny of *Aquilegia*: the biogeographical and ecological patterns of two simultaneous but contrasting radiations. *Plant Systematics and Evolution*, **284**, 171-185.

Box MS, Dodsworth S, Rudall PJ, Bateman RM, Glover BJ. 2011. Characterization of *Linaria* *KNOX* genes suggests a role in petal-spur development. *The Plant Journal*, **68**, 703-714.

Box MS, Dodsworth S, Rudall PJ, Bateman RM, Glover BJ. 2012. Flower-specific *KNOX* phenotype in the orchid *Dactylorhiza fuchsii*. *Journal of Experimental Botany*, **63**, 4811-4819.

Brown WH. 1938. The bearing of nectaries on the phylogeny of flowering plants. *Proceedings of the American Philosophical Society*, **79**, 549-570+572-595.

Chapman EJ, Estelle M. 2009. Mechanism of auxin-regulated gene expression in plants. *Annual Review of Genetics*, **43**, 265-285.

Darwin C. 1862. *The Various Contrivances by which Orchids are Fertilized by Insects*. London: John Murray.

Fernández-Mazuecos M, Blanco-Pastor JL, Juan A, Carnicero P, Forrest A, Alarcón M, Vargas P, Glover BJ. 2019. Macroevolutionary dynamics of nectar spurs, a key evolutionary innovation. *New Phytologist*, **222**, 1123-1138.

Finet C, Berne-Dedieu A, Scutt CP, Marlétaz F. 2012. Evolution of the ARF gene family in land plants: old domains, new tricks. *Molecular Biology and Evolution*, **30**, 45-56.

Fior S, Li M, Oxelman B, Viola R, Hodges SA, Ometto L, Varotto C. 2013. Spatiotemporal reconstruction of the *Aquilegia* rapid radiation through next-generation sequencing of rapidly evolving cpDNA regions. *New Phytologist*, **198**, 579-592.

Galun E. 2010. *Phytohormones and Patterning: The Role of Hormones in Plant Architecture*. Singapore: World Scientific Pub Co Inc.

Golz JF, Keck EJ, A H. 2002. Spontaneous mutations in *KNOX* genes give rise to a novel floral

structure in *Antirrhinum*. *Current Biology*, **12**, 515-522.

Gould B, Kramer EM. 2007. Virus-induced gene silencing as a tool for functional analyses in the emerging model plant *Aquilegia* (columbine, Ranunculaceae). *Plant Methods*, **3**, 6.

Guilfoyle TJ, Hagen G. 2007. Auxin response factors. *Current Opinion in Plant Biology*, **10**, 453-460.

Guindon S, Dufayard JF, Lefort V, Anisimova M, Hordijk W, Gascuel O. 2010. New algorithms and methods to estimate maximum-likelihood phylogenies: assessing the performance of PhyML 3.0. *Systematic Biology*, **59**, 307-321.

Hodges SA. 1997a. Floral nectar spurs and diversification. *International Journal of Plant Sciences*, **158**, S81-S88.

Hodges SA. 1997b. A rapid radiation due to a key innovation in columbines. In Givinish T & Sytsma K, eds. *Molecular Evolution and Adaptive Radiation*. Cambridge: Cambridge University Press, 391-405.

Hodges SA, Arnold ML. 1994. Columbines: a geographically widespread species flock. *Proceedings of the National Academy of Sciences of the United States of America*, **91**, 5129-5132.

Hodges SA, Arnold ML. 1995. Spurring plant diversification: are floral nectar spurs a key innovation? *Proceedings of the Royal Society B: Biological Sciences*, **262**, 343-348.

Javelle M, Timmermans MC. 2012. In situ localization of small RNAs in plants by using LNA probes. *Nature Protocols*, **7**, 533-541.

Kramer EM. 2005. Methods for studying the evolution of plant reproductive structures: comparative gene expression techniques. *Methods in Enzymology*, **395**, 617-636.

Kramer EM, Hodges SA. 2010. *Aquilegia* as a model system for the evolution and ecology of petals. *Philosophical Transactions of the Royal Society B: Biological Sciences*, **365**, 477-490.

Kramer EM, Holappa L, Gould B, Jaramillo MA, Setnikov D, Santiago PM. 2007.

Elaboration of B gene function to include the identity of novel floral organs in the lower eudicot *Aquilegia*. *The Plant Cell*, **19**, 750-766.

Kumar S, Stecher G, Tamura K. 2016. MEGA7: molecular evolutionary genetics analysis

version 7.0 for bigger datasets. *Molecular Biology and Evolution*, **33**, 1870-1874.

Kuusk S, Sohlberg JJ, Magnus Eklund D, Sundberg E. 2006. Functionally redundant SHI family genes regulate Arabidopsis gynoecium development in a dose-dependent manner.

The Plant Journal **47**, 99-111.

Lee JY, Baum SF, Oh SH, Jiang CZ, Chen JC, Bowman JL. 2005. Recruitment of *CRABS CLAW* to promote nectary development within the eudicot clade. *Development*, **132**, 5021-5032.

Lin IW, Sosso D, Chen LQ, Gase K, Kim SG, Kessler D, Klinkenberg PM, Gorder MK, Hou BH, Qu XQ, et al. 2014. Nectar secretion requires sucrose phosphate synthases and the sugar transporter SWEET9. *Nature*, **508**, 546-549.

Liu N, Wu S, Van Houten J, Wang Y, Ding B, Fei Z, Clarke TH, Reed JW, van der Knaap E. 2014. Down-regulation of *AUXIN RESPONSE FACTORS 6* and *8* by microRNA 167 leads to floral development defects and female sterility in tomato. *Journal of Experimental Botany*, **65**, 2507-2520.

Livak KJ, Schmittgen TD. 2001. Analysis of relative gene expression data using real-time quantitative PCR and the $2^{-\Delta\Delta CT}$ Method. *Methods*, **25**, 402-408.

Min Y, Bunn JI, Kramer EM. 2018. Homologs of the *STYLISH* gene family control nectary development in *Aquilegia*. *New Phytologist*, **221**, 1090-1100.

Min Y, Kramer EM. 2016. The *Aquilegia JAGGED* homolog promotes proliferation of adaxial cell types in both leaves and stems. *New Phytologist*, **216**, 536-548.

Moyroud E, Glover BJ. 2017. The evolution of diverse floral morphologies. *Current Biology*, **27**, R941-R951.

Munz PA. 1946. *Aquilegia*: The cultivated and wild Columbines. *Gentes herbarum*, **7**, 1-150.

Mutte SK, Kato H, Rothfels C, Melkonian M, Wong GK, Weijers D. 2018. Origin and evolution of the nuclear auxin response system. *eLife*, **7**, e33399.

Nagpal P, Ellis CM, Weber H, Ploense SE, Barkawi LS, Guilfoyle TJ, Hagen G, Alonso JM, Cohen JD, Farmer EE, et al. 2005. Auxin response factors ARF6 and ARF8 promote jasmonic acid production and flower maturation. *Development*, **132**, 4107-4118.

Petersen M, Wengel J. 2003. LNA: a versatile tool for therapeutics and genomics. *Trends in*

Biotechnology, **21**, 74-81.

Puzey JR, Gerbode SJ, Hodges SA, Kramer EM, Mahadevan L. 2011. Evolution of spur-length diversity in *Aquilegia* petals is achieved solely through cell-shape anisotropy.

Proceedings of the Royal Society B: Biological Sciences, **279**, 1640-1645.

Puzey JR, Kramer EM. 2009. Identification of conserved *Aquilegia coerulea* microRNAs and their targets. *Gene*, **448**, 46-56.

Radhika V, Kost C, Boland W, Heil M. 2010. The role of jasmonates in floral nectar secretion.

PLoS One, **5**, e9265.

Reeves PH, Ellis CM, Ploense SE, Wu MF, Yadav V, Tholl D, Chetelat A, Haupt I,

Kennerley BJ, Hodgens C, et al. 2012. A regulatory network for coordinated flower maturation. *PLoS Genetics*, **8**, e1002506.

Remington DL, Vision TJ, Guilfoyle TJ, Reed JW. 2004. Contrasting modes of diversification

in the *Aux/IAA* and *ARF* gene families. *Plant Physiology*, **135**, 1738-1752.

Sharma B, Guo C, Kong H, Kramer EM. 2011. Petal-specific subfunctionalization of an

APETALA3 paralog in the Ranunculales and its implications for petal evolution. *New Phytologist*, **191**, 870-883.

Sharma B, Kramer EM. 2013. Virus-induced gene silencing in the rapid cycling columbine

Aquilegia coerulea "Origami". In Bekcer P, eds. *Virus-Induced Gene Silencing: Methods and Protocols*. New York: Springer Science + Business Media, 71-81.

Szécsi J, Joly C, Bordji K, Varaud E, Cock JM, Dumas C, Bendahmane M. 2006.

BIGPETALp, a *bHLH* transcription factor is involved in the control of Arabidopsis petal size.

The EMBO Journal, **25**, 3912-3920.

Tabata R, Ikezaki M, Fujibe T, Aida M, Tian CE, Ueno Y, Yamamoto KT, Machida Y,

Nakamura K, Ishiguro S. 2010. Arabidopsis Auxin Response Factor6 and 8 regulate jasmonic acid biosynthesis and floral organ development via repression of class 1 *KNOX* genes. *Plant & Cell Physiology*, **51**, 164-175.

Tucker SC, Hodges SA. 2005. Floral ontogeny of *Aquilegia*, *Semiaquilegia*, and *Enemion*

(Ranunculaceae). *International Journal of Plant Sciences*, **166**, 557-574.

-
- Ulmasov T, Hagen G, Guilfoyle TJ. 1999a.** Activation and repression of transcription by auxin-response factors. *Proceedings of the National Academy of Sciences of the United States of America*, **96**, 5844-5849.
- Ulmasov T, Hagen G, Guilfoyle TJ. 1999b.** Dimerization and DNA binding of auxin response factors. *The Plant Journal*, **19**, 309-319.
- Varaud E, Brioudes F, Szécsi J, Leroux J, Brown S, Perrot-Rechenmann C, Bendahmane M. 2011.** AUXIN RESPONSE FACTOR8 regulates *Arabidopsis* petal growth by interacting with the bHLH transcription factor BIGPETALp. *The Plant Cell*, **23**, 973-983.
- Vernoux T, Brunoud G, Farcot E, Morin V, Van den Daele H, Legrand J, Oliva M, Das P, Larrieu A, Wells D, et al. 2011.** The auxin signalling network translates dynamic input into robust patterning at the shoot apex. *Molecular Systems Biology*, **7**, 508.
- Whittall JB, Hodges SA. 2007.** Pollinator shifts drive increasingly long nectar spurs in columbine flowers. *Nature*, **447**, 706-709.
- Wu MF, Tian Q, Reed JW. 2006.** *Arabidopsis microRNA167* controls patterns of *ARF6* and *ARF8* expression, and regulates both female and male reproduction. *Development*, **133**, 4211-4218.
- Yant L, Collani S, Puzey J, Levy C, Kramer EM. 2015.** Molecular basis for three-dimensional elaboration of the *Aquilegia* petal spur. *Proceedings of the Royal Society B: Biological Sciences*, **282**, 20142778.
- Zhu RR, Gao YK, Zhang QX. 2014.** Quantitative trait locus mapping of floral and related traits using an F₂ population of *Aquilegia*. *Plant Breeding*, **133**, 153-161.

Table 1. Yeast two-hybrid (Y2H) results for the AqARF6, AqARF8, AqSHY2, and AqBPE proteins in *Aquilegia coerulea*.

AD \ BK	AqARF6	AqARF8	AqSHY2	AqBPE
AqARF6	-	+	+	-
AqARF8	-	+	+	-
AqSHY2	-	+	-	-
AqBPE	-	-	-	-

AD and BK indicates the yeast cotransformed with corresponding constructs that were used as prey and bait, respectively. + indicates the interactions between two proteins, while - represents the lack of interaction, which is based on the results from -AHLT SD media supplemented with 10 mM 3-AT.

Fig. Legends

Fig. 1. Development of the petal spurs of *Aquilegia coerulea* and gene expression patterns for *AqARF6* and *AqARF8* assayed by RT-qPCR.

(a-e) Morphological features of the petal spur at different stages of floral development. (a) Inflorescence in which the terminal flower shows slightly protruding spur cups. (b) Stage F1 flower in which the spurs reach a length of 0.2 – 0.4 cm, consistent with the cell proliferation phase of spur development. (c) Stage F2 flower in which the spurs are 0.5 – 0.9 cm, covering the phase of transition between cell division and cell expansion. (d) Stage F3 flowers with spurs having a length of 1.5 – 2.0 cm, indicative of the cell elongation phase. (e) Stage F4 flowers that are fully open and have spurs achieving their final length. (f-g) RT-qPCR results for *AqARF6* (f) and *AqARF8* (g) genes from dissected sepals (Se), petal blades (Pe_b) and petal spurs (Pe_sp) corresponding to stages F1 to F4. Additional reactions were performed from seedlings (Sdl), pre-vernalized vegetative leaves (Le), and inflorescences (Inf), as well as pooled stamens (St),

staminodia (Std) and carples (Ca) from stages F1 to F4. For each tissue type, four biological replicates were tested. Error bars represent standard deviations from three technical replicates. Scale bars = 0.5 cm.

Fig. 2. Locked nucleic acid (LNA) *in situ* hybridization of *AqARF6* and *AqARF8* in *Aquilegia coerulea*.

(a-d) Expression patterns of *AqARF6* from floral meristems at stage 3 (a), stage 6 (b), stage 9 (c) and petals at stage 11 (d). (e-h) Expression patterns of *AqARF8* from floral meristems at stage 3 (e), stage 6 (f), stage 9 (g) and petals at stage 11 (h). Black arrowheads indicate petal primordia. Scale bars = 100 μ m.

Fig. 3. *AqARF8* and *AqARF6* silenced *Aquilegia coerulea* flowers show significantly shorter petal spurs.

(a-b) Strongly TRV2-*AqANS* silenced flowers (*ans_s*) shown in front (a) and side (b) views, respectively. (c) Side view of a partially TRV2-*AqANS* silenced flower. (d) Side view of a wild type (WT) flower. (e-f) Strongly TRV2-*AqARF8-AqARF6-AqANS* silenced flowers (*arf_s*) shown in front (e) and side (f) view, respectively. (g) Side view of a partially TRV2-*AqARF8-AqARF6-AqANS* silenced flower. (h) Comparison among WT, *ans_s*, *arf_m* and *arf_s* petals. (i-l) Measurements and statistical analyses of petal width (i), petal length (j), petal blade length (k) and petal spur length (l) for WT petals and *ARF*-silenced petals showing *arf_s*, *arf_m*, and unsilenced phenotypes (*arf_u*). Error bars represent standard deviation. White arrowheads in (c) and (g) indicate the strong phenotypes of petals in a partially silenced flower. Scale bars = 1 cm.

Fig. 4. Shorter petal spurs in *Aquilegia coerulea* *AqARF6* and *AqARF8*-silenced petals can be attributed to decreased cell length and anisotropy.

(a-b) Cell features in WT (a) and *arf_s* (b) petals. Insets images a1/b1, a2/b2, and a3/b3 show the magnified light microscope images that highlighted with the yellow rectangles in (a) and (b). Note that identical lengths of the fields of 270 μ m were selected for easy comparison. Horizontal and

vertical lines in a3 and b3 indicate the cell length (l) and width (w), respectively. (c-f) Statistical analyses of the total cell number (c), accumulative cell length (d), average cell length (e) and average cell anisotropy (ϵ) (f) from blade apex through spur apex between WT and strongly *arf_s* petals. Error bars represent standard deviation. (g-h) Variation in average length (g) and cell anisotropy (ϵ) (h) across bins of 20 cells from the blade apex through the spur apex between WT and *arf_s* petals, with spur lengths normalized to 1.0. Light grey and blue shading represents standard deviation of the measurements from three each of wildtype and silenced petals. Scale bars = 1 cm.

Fig. 5. Silencing of *AqARF6* and *AqARF8* in *Aquilegia coerulea* results in loss of nectar production.

(a, c) Nectar accumulated within WT (a) and *ans_s* (c) petal spurs. White arrowhead indicates the relative position of accumulated nectar within the spur. (b, d) Longitudinal free-hand section through the spur shows nectar at the apex of a wildtype (WT) (b) and *AqANS*-silenced (*ans_s*) (d) petal spur. (e-f) No nectar production was observed within *arf_s* petal spurs. (g) Comparison of the accumulated nectar in terms of the percent of spur length occupied in WT, *ans_s*, *arf_s*, *arf_m* and *arf_u* petals, which are represented by light gray, gray, light blue, blue, and dark blue bars, respectively. (h-j) Scanning electron microscopy (SEM) of the WT petal spur apex showing the outer surface (h), internal nectary tissue (i) and internal extruded secretory residues (j). (k) Histological section of nectary tissue of WT petal spur. Green box indicates magnified cell organization of the underlying parenchyma. (l-n) SEM of *arf_s* petal spur apex showing the outer surface (l), internal nectary tissue (m) and internal surface without secretory residue (n). (o) Histological section of nectary tissue of *arf_s* petal spur. Green box indicates magnified cell organization of the underlying parenchyma. (p-r) Relative expression levels of *AqSTY1* (p), *AqSTY2* (q) and *AqLRP* (r) in WT, *ans_s*, *arf_m*, and *arf_s* petals, which are represented by light gray, gray, blue, and light blue bars, respectively. Error bars represent standard deviation of three biological replicates from (WT) and *ans_s* flowers, and technical replicates of individual *arf*-silenced petals. Scale bars = 1 cm (a, c, e) and 100 μ m (h-o).

Supporting Information

Fig. S1. Gene structures of *AqARF6* and *AqARF8* in *A. coerulea*.

Fig. S2. Alignment of conserved motifs of ARF6-like and ARF8-like proteins.

Fig. S3. Phylogenetic relationships of *ARF6*- and *ARF8*-like genes.

Fig. S4. RT-qPCR analyses of silenced sepals and petals in *A. coerulea*.

Fig. S5. Phenotypes of the sepal, stamen, staminode, and carpel in *ARF*-silenced *A. coerulea* flowers.

Fig. S6. Cell width and area changes in *A. coerulea* *ARF6/8*-silenced petals.

Fig. S7. *BIGPETAL*-like genes.

Fig. S8. Interactions among *A. coerulea* proteins of *AqARF6*, *AqARF8*, *AqSHY2*, and *AqBPE* genes as revealed by using Y2H assays in *A. coerulea*.

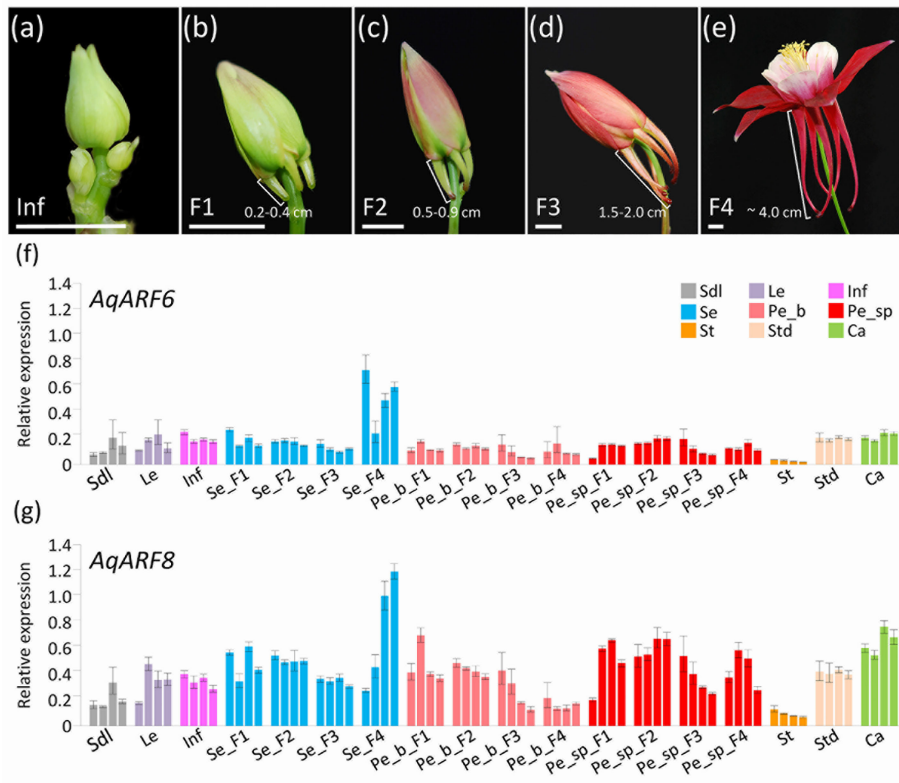
Fig. S9. Exogenous application of IAA on *A. coerulea* petals resulted in disruption in laminar organization.

Fig. S10. Jasmonic acid has no obvious effect on nectar production in *A. coerulea*.

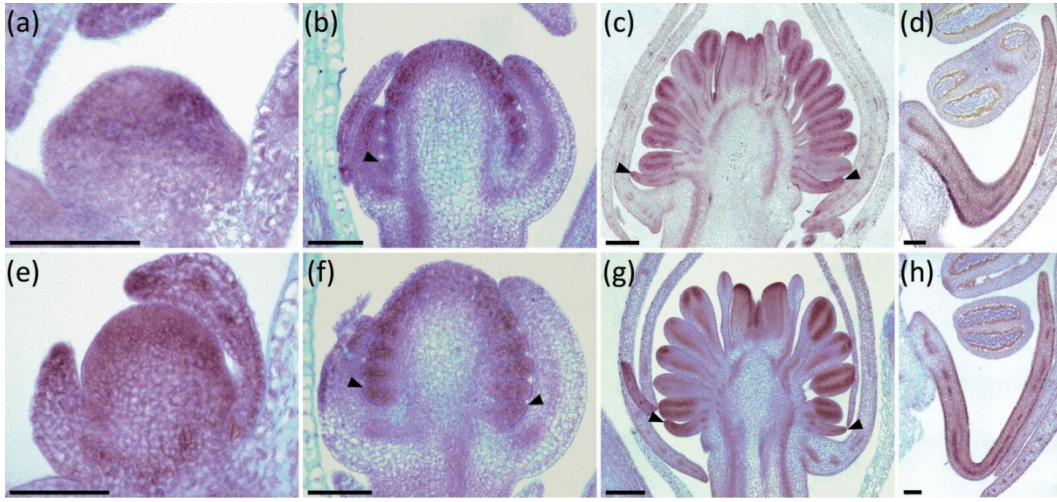
Table S1. Information on primers used in this study

Table S2. Information on *ARF*-like genes used for phylogenetic analysis in this study

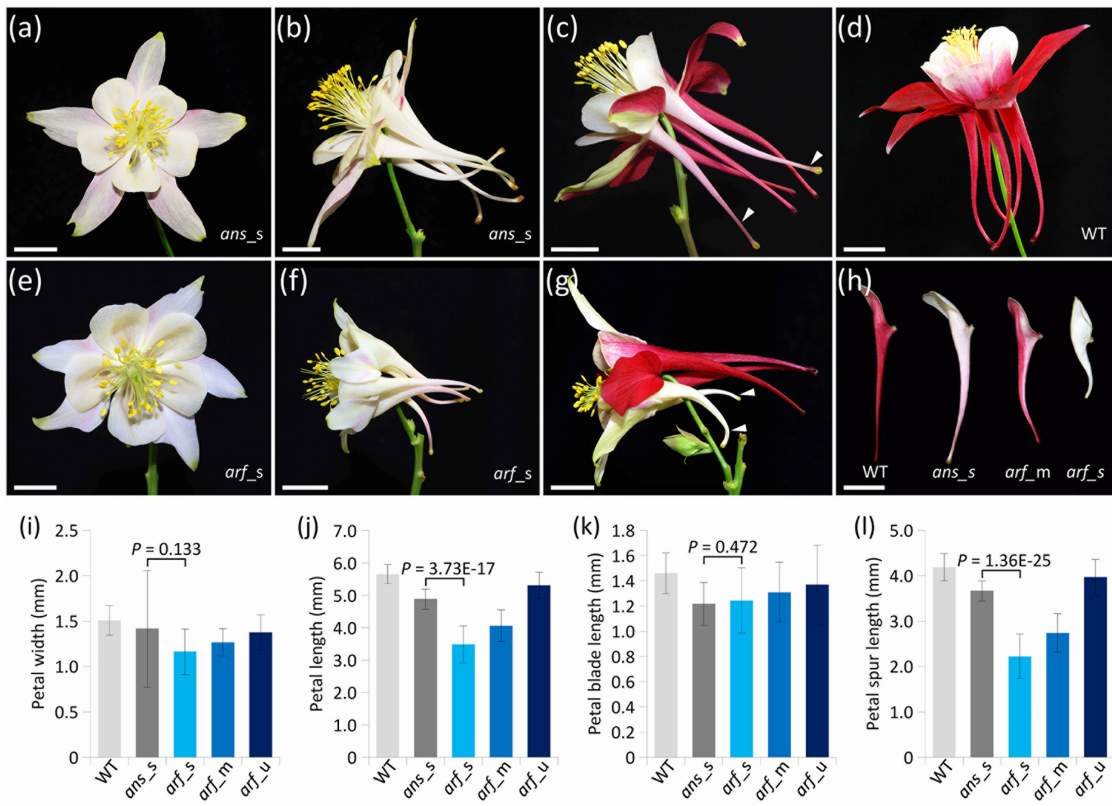
Table S3. Information on *BPE*-like genes used for phylogenetic analysis in this study



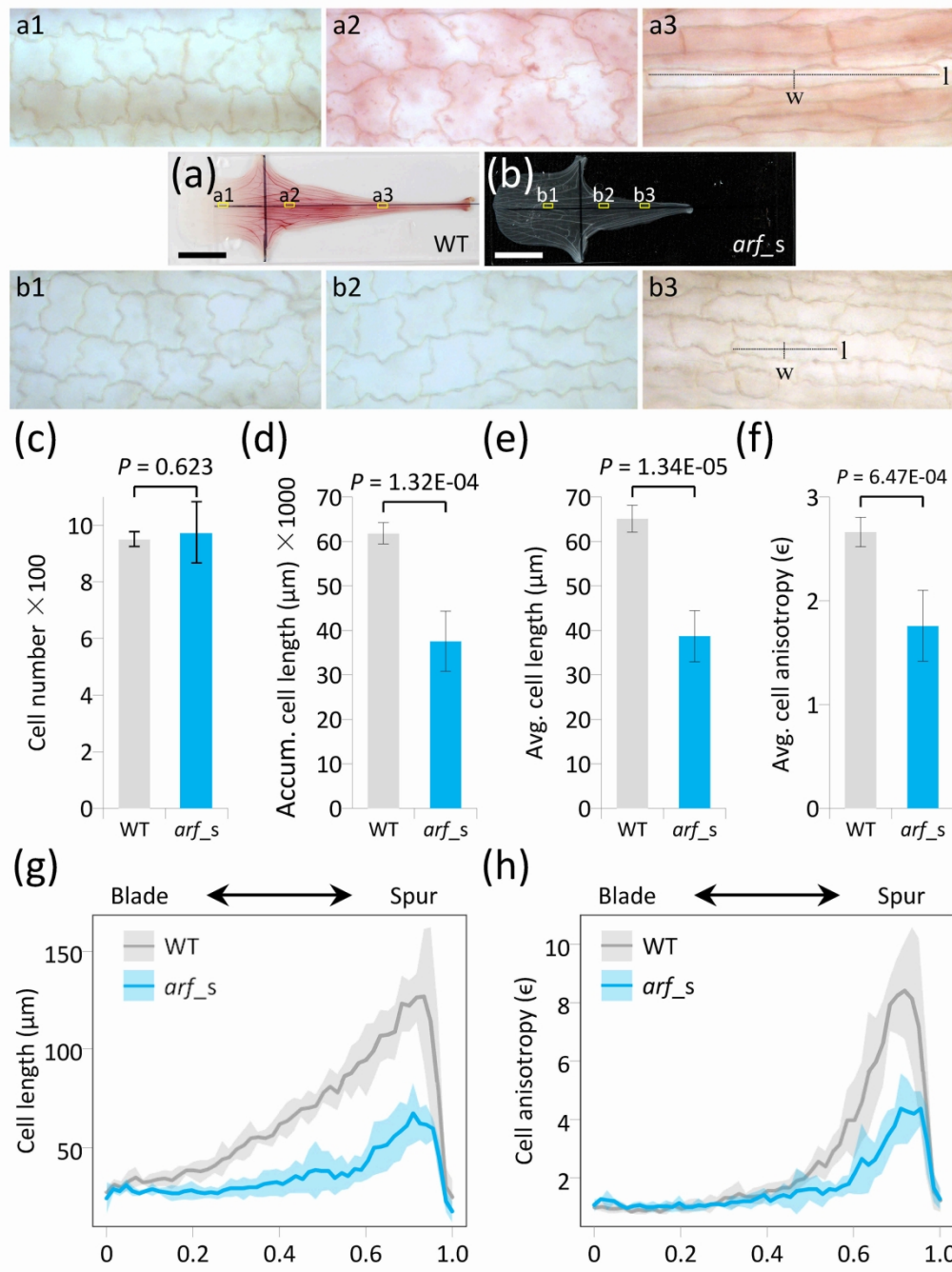
nph_16633_f1.jpg



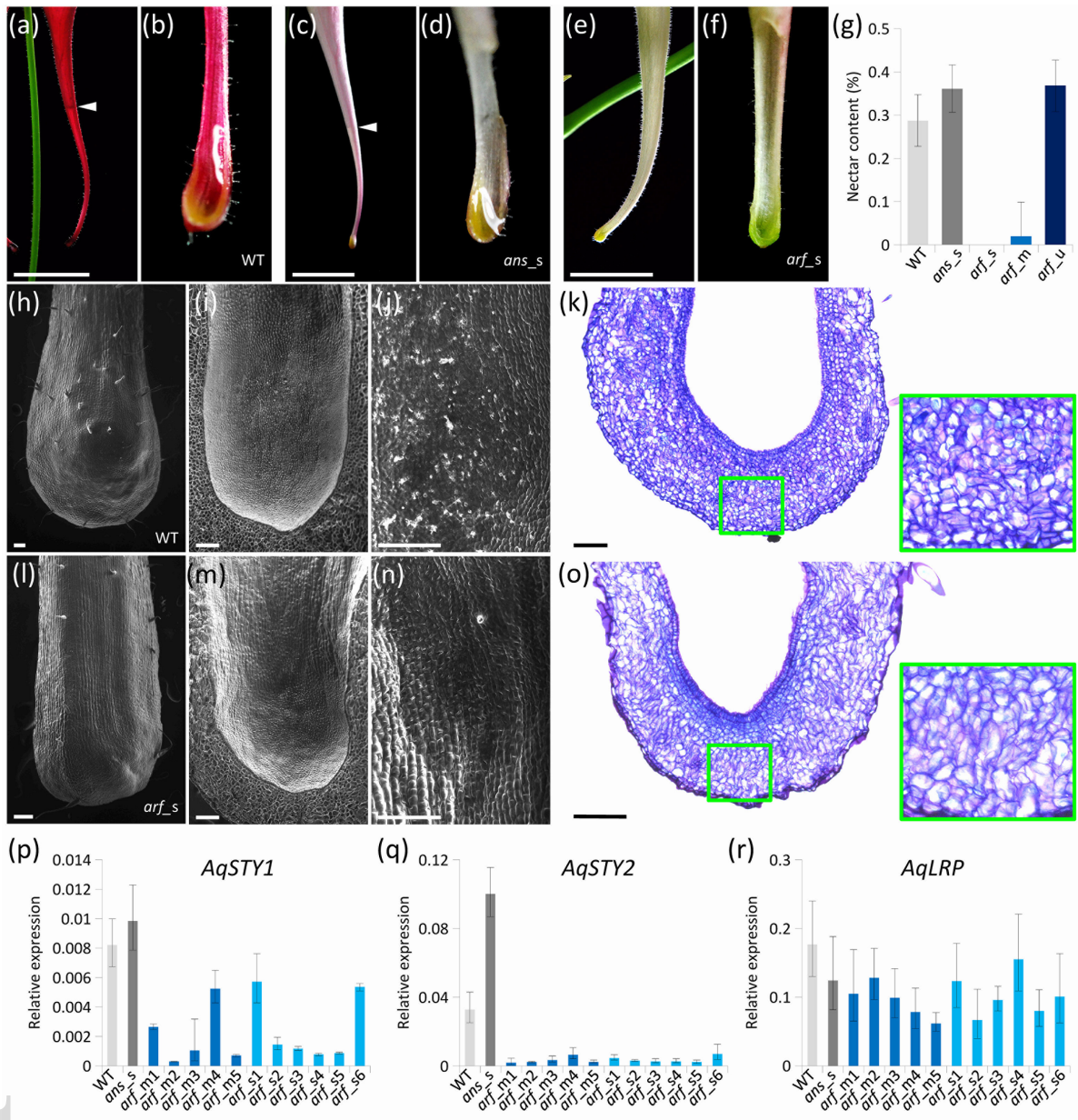
nph_16633_f2.jpeg



nph_16633_f3.jpg



nph_16633_f4.jpg



nph_16633_f5.jpg